The Journal of Toxicological Sciences (J. Toxicol. Sci.)
Vol.41, No.1, 105-113, 2016

Original Article

Arsenic acid inhibits proliferation of skin fibroblasts, and increases cellular senescence through ROS mediated MST1-FOXO signaling pathway

Yuya Yamaguchi[1], Harishkumar Madhyastha[1], Radha Madhyastha[1], Narantsog Choijookhuu[2], Yoshitaka Hishikawa[2], Yutthana Pengjam[1,3], Yuichi Nakajima[1] and Masugi Maruyama[1]

[1]Department of Applied Physiology, Faculty of Medicine, University of Miyazaki, Miyazaki 889-1692, Japan
[2]Department of Anatomy, Histochemistry and Cell biology, Faculty of Medicine, University of Miyazaki, Miyazaki 889-1692, Japan
[3]Faculty of Medical Technology, Prince of Songkla University, HatYai, Songkhla, Thailand

(Received September 2, 2015; Accepted November 18, 2015)

ABSTRACT — Arsenic exposure through drinking water is a major public health problem. It causes a number of toxic effects on skin. Arsenic has been reported to inhibit cell proliferation in *in vitro* conditions. However, reports about the molecular mechanisms are limited. Here, we investigated the mechanism involved in arsenic acid-mediated inhibition of cell proliferation using mouse skin fibroblast cell line. The present study found that 10 ppm arsenic acid inhibited cell proliferation, without any effect on cell death. Arsenic acid induced the generation of reactive oxygen species (ROS), resulting in oxidative stress to DNA. It also activated the mammalian Ste20-like protein kinase 1 (MST1); however the serine/threonine kinase Akt was downregulated. Forkhead box O (FOXO) transcription factors are activated through phosphorylation by MST1 under stress conditions. They are inhibited by phosphorylation by Akt through external and internal stimuli. Activation of FOXOs results in their nuclear localization, followed by an increase in transcriptional activity. Our results showed that arsenic induced the nuclear translocation of FOXO1 and FOXO3a, and altered the cell cycle, with cells accumulating at the G2/M phase. These effects caused cellular senescence. Taken together, our results indicate that arsenic acid inhibited cell proliferation through cellular senescence process regulated by MST1-FOXO signaling pathway.

Key words: Arsenic acid, Cell proliferation, Oxidative stress, Mammalian Ste20-like protein kinase 1, Forkhead box O transcription factors, Cellular senescence

INTRODUCTION

Arsenic is a naturally occurring substance that exists in practically all environments, such as air, soil, and water. The major exposure route of arsenic is through contaminated drinking water (Mandal and Suzuki, 2002). Arsenic exposure is associated with skin, lung, and bladder cancer (Wu *et al*., 1989; Huang *et al*., 1999; Simeonova and Luster, 2000; Bode and Dong, 2002; Dong, 2002); non-cancer effects include skin lesion, hypertension, diabetes, cardiovascular disease, and neurologic disorders (Yoshida *et al*., 2004; Moon *et al*., 2012). Interestingly, arsenic trioxide has been used in traditional Chinese medicine. Research works show that arsenic trioxide can induce apoptosis in human leukemia (Chen *et al*., 1997) and inhibit cell proliferation in human breast cancer cells (Chow *et al*., 2004). The molecular mechanisms of arsenic-induced inhibition of cell proliferation are not fully known. Arsenic exposure leads to the generation of reactive oxygen species (ROS) and oxidative damage to DNA (Ho *et al*., 2000; Wu *et al*., 2001; Rossman, 2003). Arsenic exposure disrupts the redox balance and produces higher level of ROS in cells, through modulation of intracellular antioxidant activities, such as decreased catalase activity and increased superoxide dismutase activity, which lead to enhanced oxidative stress (Lee and Ho, 1995). Moreover, intracellular ROS mediate multiple cellular responses. The serine/threonine protein kinase Akt, also known as protein kinase B, mediates various cellular processes such as growth, differentiation, survival, and

Correspondence: Masugi Maruyama (E-mail: masugi@med.miyazaki-u.ac.jp)

metabolism (Birkenkamp and Coffer, 2003). The downstream targets of Akt include the Forkhead box O (FOXO) transcription factors, FOXO1, FOXO3a, FOXO4, and FOXO6 (Biggs *et al*., 1999; Brunet *et al*., 1999; Kops *et al*., 1999; Nakae *et al*., 1999).

FOXOs are involved in multiple signaling pathways, affecting several physiological and pathological processes, such as apoptosis, proliferation, metabolism, aging, and tumorigenesis (Ho *et al*., 2008; Fu and Tindall, 2008). Subcellular localization of FOXOs plays a major role in the regulation of their activities and functions (Zanella *et al*., 2008). Akt has been shown to modulate the phosphorylation of FOXOs, causing the sequestration of FOXOs from transactivating their target genes (Biggs *et al*., 1999; Nakae *et al*., 1999; Brunet *et al*., 1999; Kops, 1999). Another kinase implicated in oxidative stress-induced phosphorylation of FOXO is mammalian Ste20-like protein kinase 1 (MST1). During oxidative stress, MST1 phosphorylates FOXO1 and FOXO3a at residues Ser212 and Ser207, respectively, which results in their translocation into the nucleus, enabling them to modulate target gene expressions (Lehtinen *et al*., 2006; Yuan *et al*., 2009). ROS-induced oxidative stress regulates FOXOs by altering the phosphorylation sites. We examined the signaling link between MST1 and FOXOs in cell proliferation inhibition caused by exposure to arsenic.

MATERIALS AND METHODS

Reagents

Standard arsenic solution was purchased from Merck Millipore (Darmstadt, Germany). Alpha-Minimum Essential Medium (α-MEM) (Nacalai Tesque, Inc., Kyoto, Japan), fetal bovine serum (FBS), and antibiotic mixture (5 mg/mL of Penicillin, 5 mg/mL of Streptomycin, and 10 mg/mL Neomycin) (PSN) were purchased from Gibco (Tokyo, Japan). 3-(4,5-dimethythiazol2-yl)-2,5-diphenyl tetrazolium bromide (MTT) reagent was purchased from Wako Pure Chemical Industries Ltd. (Osaka, Japan). CytoTox 96® Non-Radioactive Cytotoxicity Assay Kit was from Promega Co. (Madison, WI, USA). OxiSelect™ Intracellular ROS Assay Kit was purchased from Cell Biolabs, Inc. (San Diego, CA, USA). NE-PER Nuclear and Cytoplasmic Extraction Reagent Kit was purchased from Thermo Fisher Scientific, Inc. (Pittsburgh, PA, USA). Image-IT® Fix-Perm kit was purchased from Life Technologies (Carlsbad, CA, USA). Senescence β-Galactosidase Staining Kit was purchased from Cell Signaling Technology (Beverly, MA, USA). All other reagents were purchased from Sigma Chemical Co. (St. Louis, MO, USA) or Wako Pure Chemical Industries Ltd.

Cell culture

Mouse skin fibroblast cells (m5S) were purchased from RIKEN Cell Bank (Ibaraki, Japan). Cells were cultured in α-MEM supplemented with 10% (v/v) heat inactivated FBS and 1% (v/v) PSN at humidified chamber (5% CO_2, 37°C). At semi-confluent stage, cells were treated with different concentrations of arsenic acid for 16 hr.

Cell proliferation assay

Cell proliferation was determined by MTT assay. Cells were seeded in 96-well plates at a density of 1×10^4 cells/well. Cells were treated either with different doses of arsenic acid for 16 hr, or with 10 ppm arsenic acid for different time periods. Treated cells were washed with phosphate-buffered saline (PBS). 100 μL MTT solution was added into each well, and cells were incubated at 37°C for 3 hr. Dimethyl sulfoxide was used to dissolve formazan crystals. The resulting intracellular purple formazan was quantified with a spectrophotometer at an absorbance of 570 nm (Multiskan FC, Thermo Fisher Scientific, Inc., Pittsburgh, PA, USA).

Cytotoxicity assay

Cells were seeded in 96-well plates at a density of 1×10^4 cells/well. Cells were treated with different concentrations of arsenic acid for 16 hr. Supernatants were collected to determine the amount of lactate dehydrogenase released as a result of cytotoxicity, using a CytoTox 96® Non-Radioactive Cytotoxicity Assay Kit. The assay employs the principle of the calorimetric measurement of lactate dehydrogenase, a cytosolic enzyme released into the medium upon cell lysis. The amount of enzyme released was quantified using UV-vis spectrophotometer (Multiskan FC, Thermo Fisher Scientific, Inc.) at an absorbance of 490 nm.

Quantification of intracellular reactive oxygen species (ROS) assay

Intracellular ROS was quantified by using OxiSelect™ Intracellular ROS Assay Kit. Cells were seeded in 96-well plates at a density of 1×10^4 cells/well. Following the incubation of cells with various doses of arsenic acid for 16 hr, cells were washed with Hank's Balanced Salt Solution. 10 μM dichlorofluorescein diacetate (DCFH-DA) was added to the cells at 37°C for 1 hr in the dark. Nonfluorescent DCFH-DA is converted to fluorescent dichlorofluorescein in proportion to the amount of ROS generation in cells. The fluorescence signal was quantified using a spectrofluorometer (DTX800, Beckman Coulter,

Inc., Brea, CA, USA) at excitation and emission wavelengths of 485 and 530 nm respectively.

Intracellular ROS detection by fluorescence microscopy

Intracellular ROS was detected using OxiSelect™ Intracellular ROS Assay Kit. Cells were seeded on coverslips in 6-well plates at a density of 3×10^5 cells/well. Following the incubation of cells with 10 ppm arsenic acid for 16 hr, cells were washed with PBS, and 10 µM DCFH-DA was added to cells at 37°C for 1 hr in the dark. Slides were mounted and images captured using a fluorescence microscope (BZ-9000, Keyence, Osaka, Japan) at excitation and emission wavelengths of 485 and 530 nm respectively.

Immunostaining for 8-OHdG

Cells were seeded on coverslips in 6-well plates at a density of 3×10^5 cells/well. Following the incubation of cells with 10 ppm arsenic acid for 16 hr, cells were washed with PBS, and fixed with 4% paraformaldehyde in PBS for 10 min at room temperature. Cellular endogenous peroxidase activity was blocked with 0.3% H_2O_2 in absolute methanol for 15 min and washed with PBS. Nonspecific binding sites were blocked by incubation in PBS containing 0.5 mg/mL normal goat IgG and 1% bovine serum albumin (BSA). Cells were incubated with anti-8-OHdG for 2 hr, followed by wash in 0.075% Brij® 35 in PBS and incubation with HRP-conjugated goat anti-mouse IgG for 1 hr. After washing with 0.075% Brij® 35 in PBS, cells were incubated with DAB and H_2O_2 in the presence of nickel and cobalt ions in dark. Finally, coverslips were mounted and images captured using a microscope (1X73, Olympus, Tokyo, Japan) coupled to a digital camera at × 40 magnification.

Western blotting

Cells were seeded in 6-well plates at a density of 3×10^5 cells/well. Following the incubation of cells with various doses of arsenic acid for 16 hr, total cell lysates were prepared using radioimmunoprecipitation (RIPA) buffer. Cytoplasmic and nuclear proteins were obtained using NE-PER reagent following manufacturer's instruction. Protein fractions were resuspended in sodium dodecyl sulfate-polyacrylamide gel electrophoresis (SDS-PAGE) buffer containing 2-mercaptoethanol, and boiled at 95°C for 5 min. Protein samples were subjected to SDS-PAGE in 10% polyacrylamide gel and subsequently electroblotted onto polyvinylidene fluoride membranes (GE Healthcare, Piscataway Township, NJ, USA). After blocking non-specific binding sites for 1 hr in 3% nonfat milk in Tris-Buffered Saline and 0.1% Tween 20 (TBST), membranes were incubated overnight at 4°C with specific primary antibodies. Antibodies anti-MST1, anti-Phos. MST1/2, anti-Akt, anti-Phos. Akt, anti-FOXO1, anti-FOXO3a, anti-β actin, and anti-PCNA were purchased from Cell signaling Inc. The membranes were washed in TBST and incubated further with HRP-conjugated secondary antibodies. Protein bands were detected using an enhanced ECL kit (GE Healthcare, Tokyo, Japan) with the digital imaging system (LAS4000, Fujifilm, Tokyo, Japan). Bands were measured using Image Quant TL software (GE Healthcare Life Sciences).

Immunofluorescence studies

Cells were seeded on coverslips in 6-well plates at a density of 3×10^5 cells/well. Following the incubation of cells with 10 ppm arsenic acid for 16 hr, cells were fixed and permeabilized using Image-IT® Fix-Perm kit, following the manufacturer's protocol. After permeabilization, cells were washed with Dulbecco's PBS and non-specific binding sites were blocked in 3% BSA in Dulbecco's PBS. The coverslips were incubated overnight with anti-FOXO1 or anti-FOXO3a antibodies in Immuno Shot Reagent 1 (Cosmo Bio Co., Ltd., Tokyo, Japan) at 4°C. Cells were subsequently incubated with goat-anti-rabbit conjugated Alexa Flour® 532 (Life Technologies, Carlsbad, CA, USA) in Immuno Shot Reagent 2 (Cosmo Bio Co., Ltd.) for 1 hr. The nucleus was stained with 4',6-diamidino-2-phenylindole (DAPI) (Life Technologies). Finally, coverslips were mounted and examined under confocal microscope (TCS SP8, Leica, Wetzlar, Germany). Images were captured at × 63 magnification.

Cell cycle analysis by flow cytometer

Cells were seeded in 6-well plates at a density of 3×10^5 cells/well. Following the incubation of cells with 10 ppm arsenic acid for 16 hr, cells were fixed with 70% cold ethanol at -20°C. Following fixation, cells were stained with Guava® cell cycle reagent (Merck Millipore). Flow cytometry analysis was performed using Guava EasyCyte Mine (Millipore, Hayward, CA, USA). Flow cytometry data were analyzed using Cyto Soft version 4.2 (Millipore).

Detection of senescence associated β-galactosidase (SA-β-gal) activity

Cells were seeded on coverslips in 6-well plates at a density of 3×10^5 cells/well. Following the incubation of cells with 10 ppm arsenic acid for 16 hr, cell senescence was measured using Senescence β-Galactosidase Staining Kit following the manufacturer's protocol. Development

of a blue color was visualized under microscope (1X73, Olympus) coupled to a digital camera at × 40 magnification.

Statistical analysis

All experiments were performed in triplicate. Data are expressed as mean ± standard deviation, and the difference between the groups was analyzed by one-way ANOVA with a post hoc Dunnett's test or Student's t-test. $p < 0.05$ was considered statistically significant.

RESULTS

Effect of arsenic acid on cell proliferation and cytotoxicity in m5S cells

The effect of arsenic acid on cell proliferation was tested using MTT assay. Cells were treated with different doses of arsenic acid for 16 hr. Data showed that 10 ppm arsenic acid inhibited cell proliferation significantly ($p < 0.01$) in comparison to control (Fig. 1a). We examined the time-course effect of 10 ppm arsenic acid on cell proliferation. Results showed that 16-hr exposure to 10 ppm arsenic acid caused a significant ($p < 0.01$) inhibition in cell proliferation (Fig. 1b). Next, we studied if arsenic was cytotoxic to m5S cells, by using LDH assay. Cells were treated with various doses of arsenic acid for 16 hr. Results obtained showed that arsenic acid was not cytotoxic at any dose tested (Fig. 1c).

Arsenic acid induces intracellular ROS generation and DNA damage

Cells were treated with various doses of arsenic acid for 16 hr and tested for ROS generation using DCFH-DA. The results indicated that arsenic acid induced intracellular ROS generation in dose-dependent manner (Fig. 2a). Exposure of cells to 10 ppm arsenic acid caused an increase in fluorescence (Fig. 2b), confirming the conversion of DCFH-DA to dichlorofluorescein. We examined the expression of 8-OHdG by immunostaining to study oxidative damage to DNA. Treatment with 10 ppm arsenic acid resulted in a significantly ($p < 0.01$) large number of 8-OHdG positive cells than the control (Fig. 3). Arsenic is reported to induce ROS (You and Park, 2012). Moreover, oxidative stress has been reported to upregulate phosphorylated MST1 (Choi *et al*., 2009). We performed western blot analysis to evaluate the effect of arsenic acid on the protein expression of MST1 and Akt. Treatment with arsenic acid caused a significant increase in phosphorylated MST1 (Fig. 4a) and a decrease in phosphorylated Akt (Fig. 4b). These results implicated that arsenic acid may be promoting translocation of

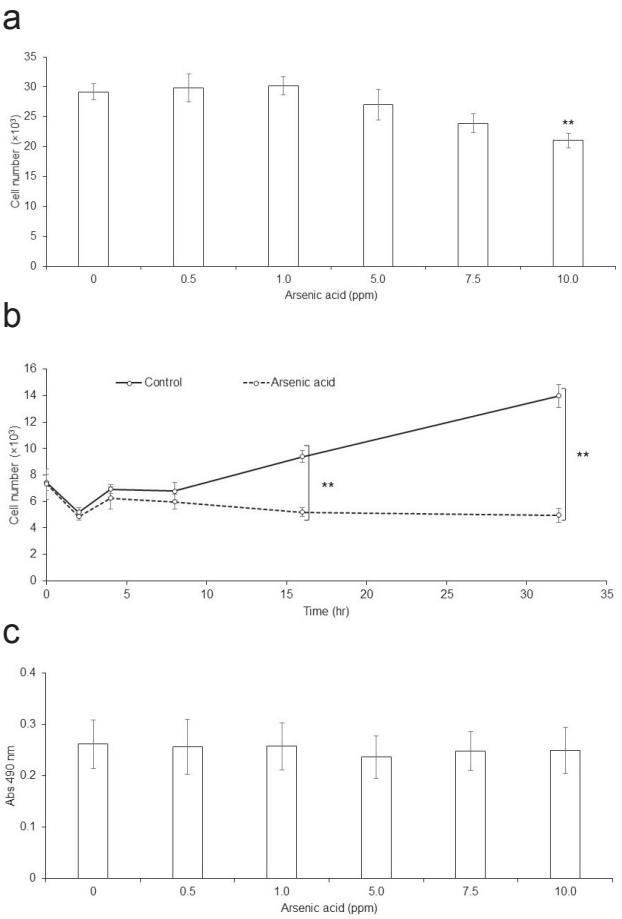

Fig. 1. Cell proliferation and cytotoxicity test. (a) Cells were treated with increasing concentrations of arsenic acid (0, 0.5, 1.0, 5.0, 7.5 and 10 ppm) for 16 hr and analyzed for cell proliferation by MTT assay. Significant (**, $p < 0.01$) decrease in cell numbers was noted in 10 ppm arsenic-treated group. (b) Cells were treated with 10 ppm arsenic acid for different time periods and analyzed for cell proliferation by MTT assay. Arsenic-treated group showed no increase in cell number up to 35 hr, whereas control group displayed significant increase (**, $p < 0.01$) from 16 hr onwards. (c) Cells treated with increasing concentrations of arsenic acid (0, 0.5, 1.0, 5.0, 7.5 and 10 ppm) for 16 hr were analyzed for cytotoxicity by measuring the amount of LDH released into medium. Arsenic acid showed no cytotoxicity effect up to 10 ppm. Data represent mean ± S.D. of three independent experiments.

FOXO from cytoplasm to the nucleus. Subcellular localizations of FOXO1 and FOXO3a were determined by confocal microscopy and western blot analysis. In untreated cells, FOXO1 and FOXO3a were localized in the cytoplasm. However, treatment of cells with arsenic acid resulted in nuclear translocation of FOXO1 and FOXO3a,

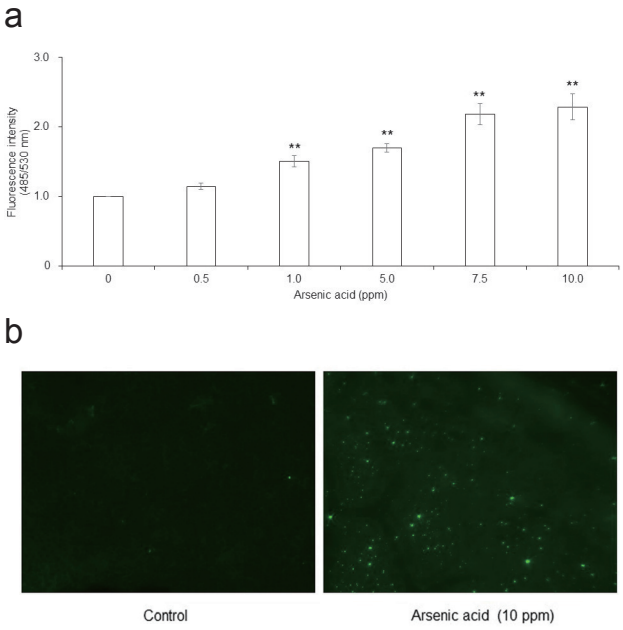

Fig. 2. Arsenic acid induces ROS generation in m5S. Cells were treated with various doses of arsenic acid for 16 hr. (a) Intracellular ROS generation was quantified by intracellular ROS assay kit using spectrofluorometer at excitation and emission of wavelengths of 485 and 530 nm respectively. Data represent mean ± S.D. of three independent experiments. **, $p < 0.01$ vs. control. (b) Intracellular fluorescence images of cells treated with 10 ppm arsenic acid. Cells with intracellular ROS are seen in fluorescent green color.

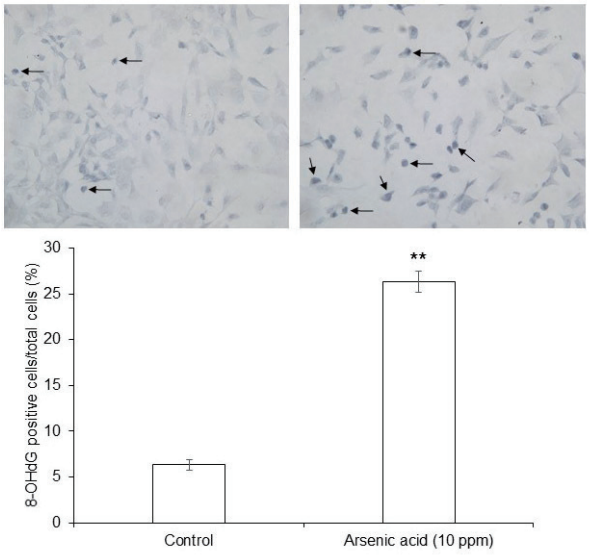

Fig. 3. Arsenic acid increases oxidative stress in m5S cells. Immunostaining was used to measure levels of the oxidative stress using stress marker 8-OHdG. The number of 8-OHdG-positive cells increased in arsenic acid (10 ppm) treated group for 16 hr compared to control. Date represent mean ± S.D. of three independent experiments. **, $p < 0.01$ vs. control. Representative images were selected as representative data from three independent experiments.

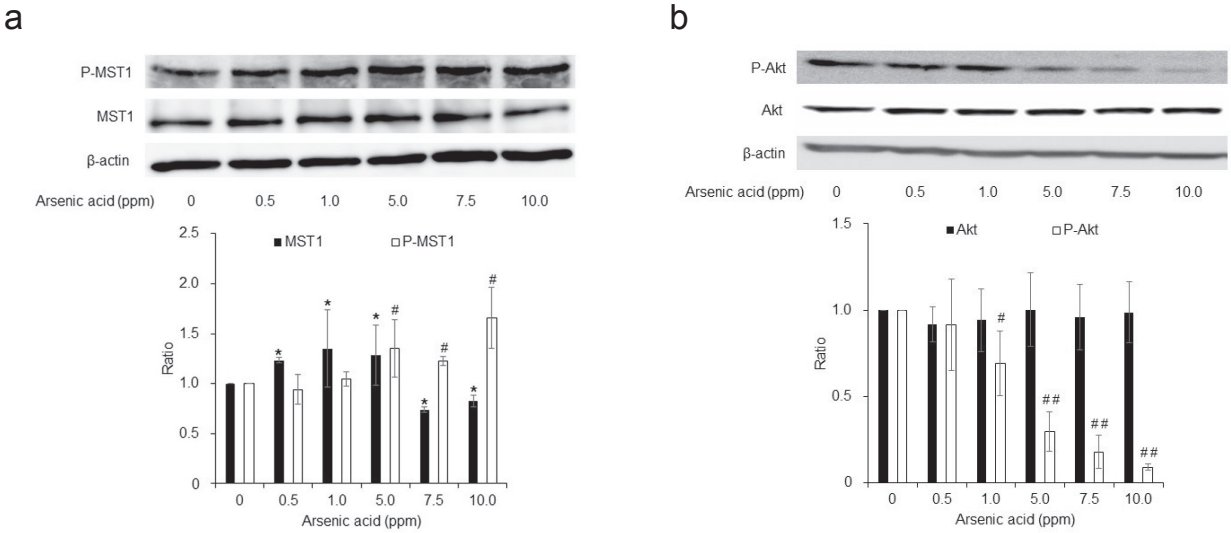

Fig. 4. Western blotting studies. Cells of m5S cells treated with increasing concentrations of arsenic acid for 16 hr were analyzed by WB for (a) phospho-MST1/2 and MST1 antibodies and (b) phospho-Akt and Akt antibodies. β-actin was used as a loading control. Data represent mean ± S.D. of three independent experiments. *, $p < 0.05$ vs. control, **, $p < 0.01$ vs. control, #, $p < 0.05$ vs. control, ##, $p < 0.01$ vs. control.

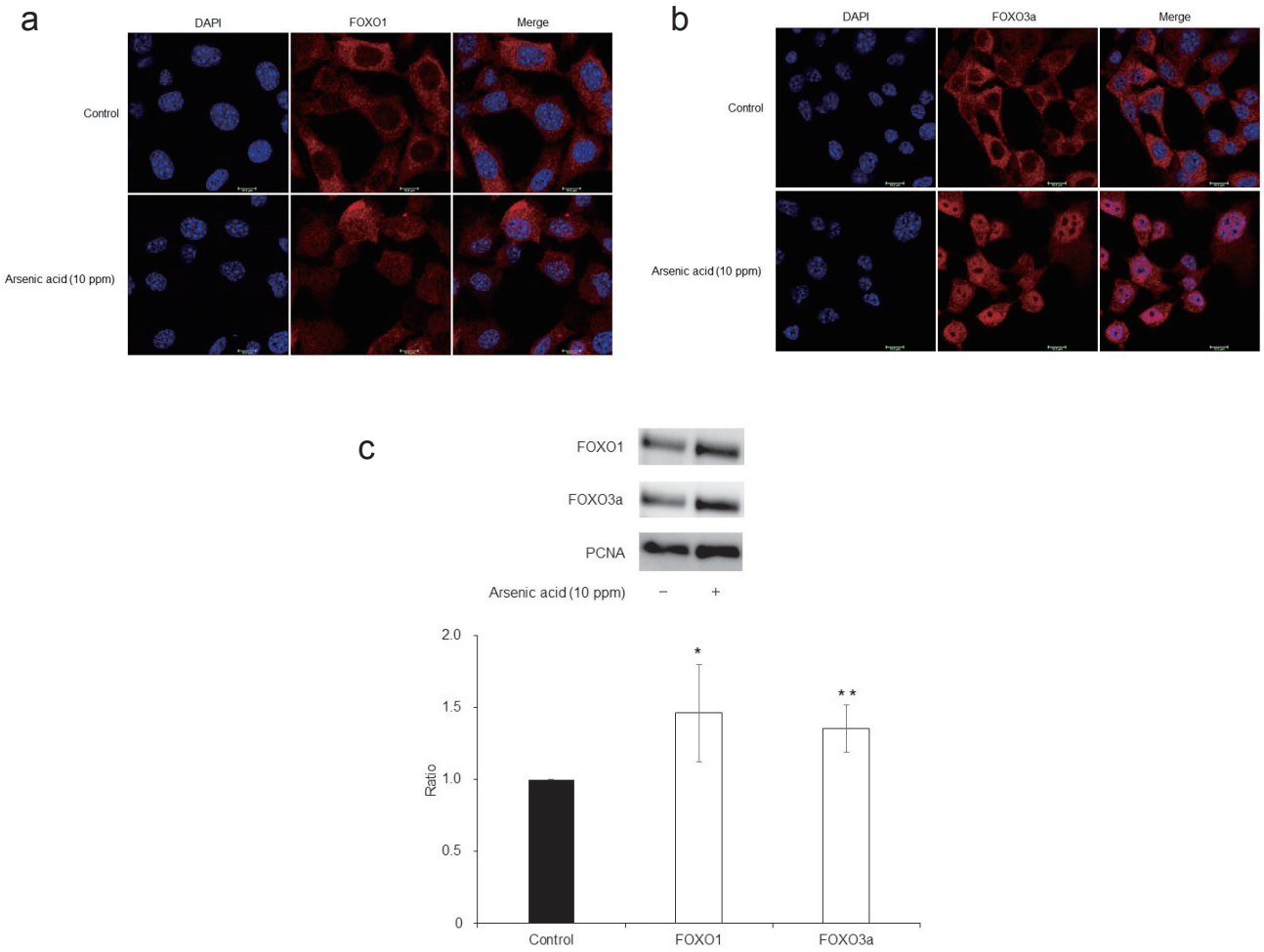

Fig. 5. Arsenic acid promotes translocation of FOXOs into nucleus. Cells were untreated or treated with 10 ppm arsenic acid for 16 hr and analyzed for FOXO1 or FOXO3a using confocal microscopy. Representative images for (a) FOXO1 (red); (b) FOXO3a (red). Nuclei were stained with DAPI (blue). (c) Quantification analysis of nuclear protein extraction by WB analysis. Proliferating cell nuclear antigen was used as nuclear protein marker. Data represent mean ± S.D. of three independent experiments. *, $p < 0.05$ vs. control, **, $p < 0.01$ vs. control.

as evidenced by immunofluorescence (Figs. 5a and 5b) and western blot of nuclear protein fractions (Fig. 5c).

Arsenic acid alters cell cycle and induces senescence

We performed flow cytometry cell cycle analysis of m5S cells exposed to 10 ppm arsenic acid. Flow cytometry analysis detected a significant decrease in G1 (58.1% in control vs. 45.0% in arsenic acid) population, with a concomitant increase in G2/M (30.3% in control vs. 40.2% in arsenic acid) in comparison with the control. The change of phase S was not statistically significant (Fig. 6). Since FOXOs have a crucial role in regulating senescence process by controlling the expression of a number of cell cycle regulators (Collado *et al*., 2000), we proceeded to study the effect of arsenic acid on cell senescence. Cells were exposed to 10 ppm arsenic acid and SA-β-gal activity was measured using the Senescence β-Galactosidase Staining Kit. Arsenic acid indeed, increased SA-β-gal activity, an indicator of cellular senescence (Fig. 7).

DISCUSSION

Arsenic is known to cause skin lesions. Skin is the first barrier of defense in disease control. Several reports

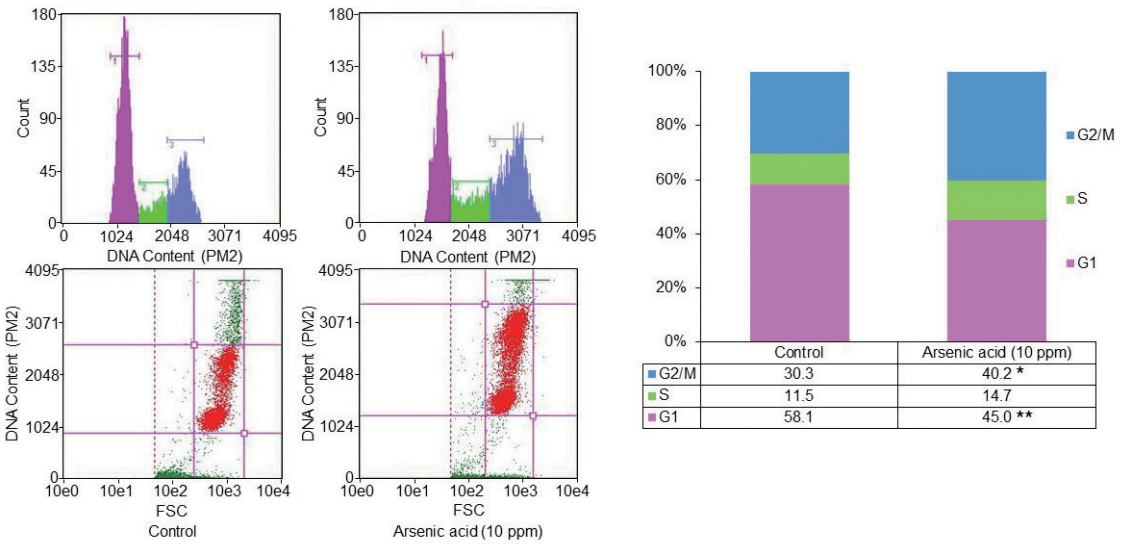

Fig. 6. Effects of arsenic acid on cell cycle distribution. Cell cycle distribution of m5S cells treated with 10 ppm arsenic acid was analyzed and quantified by FACS analysis. Data represents mean ± S.D. of three independent experiments. *, $p < 0.05$ vs. control, **, $p < 0.01$ vs. control.

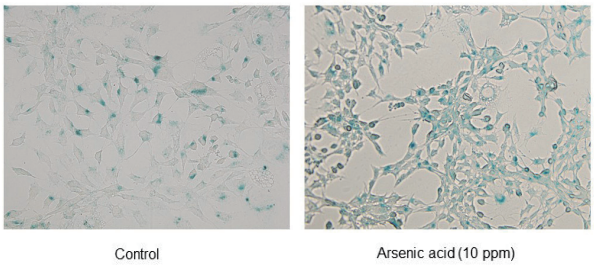

Fig. 7. Senescence analysis of fibroblast cells treated with arsenic acid. Cells were untreated or treated with 10 ppm arsenic acid for 16 hr and cell senescence was detected with the Senescence β-Galactosidase Staining Kit. Cells undergoing senescence are stained blue.

have reported inhibition of cell proliferation by exposure to arsenic (Chow *et al*., 2004). However, the molecular mechanism involved is not yet known. In this study, we examined the molecular details of the inhibitory effects of arsenic acid on cell proliferation.

Mouse skin fibroblast cells were exposed to various doses of arsenic acid for 16 hr. Cell proliferation was significantly inhibited in a dose- and time-dependent manner. However, arsenic acid was not cytotoxic at any given concentration. We showed that treatment of the fibroblast cells with arsenic acid significantly increased the generation of intracellular ROS in a dose-dependent manner. These results imply that arsenic acid can enhance oxidative stress in fibroblast cells. Overproduction or accumulation of oxygen free radicals in cells, usually referred to as oxidative stress or a pro-oxidant state, will damage DNA (Storz, 2011). We checked the oxidative damage to DNA using immunostaining for 8-OHdG. Arsenic acid, indeed, increased the number of 8-OHdG positive cells in comparison to control.

In an effort to identify the signaling pathway involved, we focused on MST1-FOXO signaling pathway in response to oxidative stress in m5S cells. MST1 mediates oxidative-stress-induced phosphorylation of FOXO1 and FOXO3a at Ser 212 and Ser 207 respectively, and promotes their translocation to nucleus (Lehtinen *et al*., 2006; Yuan *et al*., 2009). We found that exposure of cells to arsenic acid activated the expression of MST1 and also induced the translocation of FOXO1 and FOXO3a into the nucleus. Akt signaling pathway can induce phosphorylation of FOXO1 (at Thr 24, Ser 256, and Ser 319) and FOXO3a (at Thr 32, Ser 253, and Ser 315), which in turn both promotes the export of FOXOs from the nucleus and inhibits their nucleus import (Van Der Heide *et al*., 2004). Our data showed that arsenic acid downregulated the phosphorylation of Akt, thus preventing Akt-mediated export of FOXOs from the nucleus.

FOXOs play a role in cell proliferation and survival by regulating the expression of genes involved in cellular processes, such as cell cycle arrest and DNA repair. FOXO family of transcription factors gained increased

interest as pivotal elements of cell fate. It is implicated in diverse functions, from development, longevity, and aging, to control of cell survival or apoptosis (Greer and Brunet, 2005). FOXO members are directly implicated in cell cycle control, through G1-related p130 (Kops *et al*., 2002) and cyclin G2 or DNA damage-inducible gene 45α (GADD45α) (Carter and Brunet, 2007). FOXO3a has been reported to induce cell cycle arrest at G2-M checkpoint and trigger DNA repair by inducing expression of the GADD45α (Furukawa-Hibi *et al*., 2002; Tran *et al*., 2002). GADD45α induces G2 arrest by interacting with and inhibiting the kinase activity of Cdc2 suggested that the induction of GADD45α by FOXO3a in response to oxidative stress might result in G2 arrest; this is implicated in inhibition of cell growth (Jin *et al*., 2000). Therefore, we checked the cell cycle by flow cytometry. Arsenic acid reduced G1 phase cell population and increased the cell population of G2/M. Consequently, an increased population of cells were accumulated in the G2/M phase. Arsenic treatment has been shown to induce GADD45α *in vivo* (Liu *et al*., 2001) and *in vitro* (Chen *et al*., 2001). Our results are in conformation with these studies.

Cell cycle arrest is the most important factor for determining the fate of cells, and long-term stagnation with irreversible cell cycle arrest marks the beginning of senescence (Ho *et al*., 2008). Telomere-dependent senescence is a phenomenon known as the Hayflick limit (Hayflick and Moorhead, 1961). Furthermore, various cellular stresses prematurely induce the same phenotypes as replicative senescence prior to the Hayflick limit. This process is known as stress-induced premature senescence (SIPS) (Suzuki and Boothman, 2008). Age-related gene expression changes have been reported, and some of these are used as markers of senescence. SA-β-gal activity is a commonly used senescence marker. We confirmed increased SA-β-gal activity induced by arsenic acid. There is sufficient evidence implying a role for FOXO in inducing cell senescence. Reports have shown that PI3K inhibition and FOXO-induced p27 expression can induce cell cycle arrest (Collado *et al*., 2000). An *in vivo* study demonstrated the involvement of FOXO induction and PI3K repression, in oncogene-induced senescence (Courtois-Cox *et al*., 2006). Our findings that in addition to activating FOXO, arsenic also inhibited the phosphorylation of Akt, an important member of PI3K signaling pathway, is in agreement with these studies.

Taken together, our results show for the first time that arsenic acid activates MST1-FOXO signaling and subsequently triggers cellular senescence in skin fibroblast cells. These data provide a novel mechanism that inhibition of cell proliferation by arsenic acid is due to activation of MST1-FOXOs signal-mediated cellular senescence (Fig. 8).

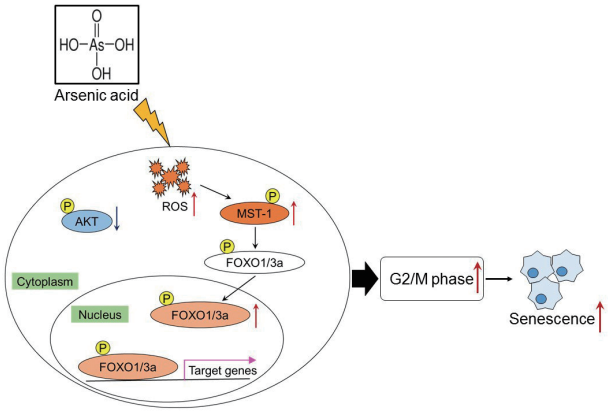

Fig. 8. Schematic flow diagram showing arsenic acid-mediated MST1-FOXO signaling in normal skin fibroblast cells. Arsenic induces intracellular ROS and leads to activation of MST1-FOXO signaling. Consequently, FOXOs translocate to nucleus and mediate cell cycle, leading to cell senescence.

ACKNOWLEDGMENTS

This research was supported by the University of Miyazaki, Japan.

Conflict of interest---- The authors declare that there is no conflict of interest.

REFERENCES

Biggs, W.H.3rd, Meisenhelder, J., Hunter, T., Cavenee, W.K. and Arden, K.C. (1999): Protein kinase B/Akt-mediated phosphorylation promotes nuclear exclusion of the winged helix transcription factor FKHR1. Proc. Natl. Acad. Sci. USA, **96**, 7421-7426.

Birkenkamp, K.U. and Coffer, P.J. (2003): FOXO transcription factors as regulators of immune homeostasis: molecules to die for? J. Immunol., **171**, 1623-1629.

Bode, A.M. and Dong, Z. (2002): The paradox of arsenic: Molecular mechanisms of cell transformation and chemotherapeutic effects. Crit. Rev. Oncol. Hematol., **42**, 5-24.

Brunet, A., Bonni, A., Zigmond, M.J., Lin, M.Z., Juo, P., Hu, L.S., Anderson, M.J., Arden, K.C., Blenis, J. and Greenberg, M.E. (1999): Akt promotes cell survival by phosphorylating and inhibiting a Forkhead transcription factor. Cell, **96**, 857-868.

Carter, M.E. and Brunet, A. (2007): FOXO transcription factors. Curr. Biol., **17**, R113-R114.

Chen, F., Lu, Y., Zhang, Z., Vallyathan, V., Ding, M., Castranova, V. and Shi, X. (2001): Opposite effect of NF-κB and c-Jun N-terminal kinase on p53-independent GADD45 Induction by arsenite. J. Biol. Chem., **276**, 11414-11419.

Chen, G.-Q., Shi, X.-G., Tang, W., Xiong, S.-M., Zhu, J., Cai, X., Han, Z.-G., Ni, J.-H., Shi, G.-Y., Jia, P.-M., Liu, M.-M., He, K.-L., Niu, C., Ma, J., Zhang, P., Zhang, T.-D., Paul, P., Naoe, T., Kitamura, K., Miller, W., Waxman, S., Wang, Z.-Y., De The, H., Chen, S.-J. and Chen, Z. (1997): Use of arsenic trioxide (As2O3) in the treatment of acute promyelocytic leukemia (APL): I. As2O3 exerts dose-dependent dual effects on APL cells. Blood, **89**, 3345-3353.

Choi, J., Oh, S., Lee, D., Oh, H.J., Park, J.Y., Lee, S.B. and Lim, D.-S. (2009): Mst1-FoxO signaling protects Naïve T lymphocytes from cellular oxidative stress in mice. PLoS One, **4**, e8011.

Chow, S.K., Chan, J.Y. and Fung, K.P. (2004): Inhibition of cell proliferation and the action mechanisms of arsenic trioxide (As2O3) on human breast cancer cells. J. Cell. Biochem., **93**, 173-187.

Collado, M., Medema, R.H., García-Cao, I., Dubuisson, M.L., Barradas, M., Glassford, J., Rivas, C., Burgering, B.M., Serrano, M. and Lam, E.W. (2000): Inhibition of the phosphoinositide 3-kinase pathway induces a senescence-like arrest mediated by p27(kip)1. J. Biol. Chem., **275**, 21960-21968.

Courtois-Cox, S., Genther Williams, S.M., Reczek, E.E., Johnson, B.W., McGillicuddy, L.T., Johannessen, C.M., Hollstein, P.E., MacCollin, M. and Cichowski, K. (2006): A negative feedback signaling network underlies oncogene-induced senescence. Cancer Cell, **10**, 459-472.

Dong, Z. (2002): The molecular mechanisms of arsenic-induced cell transformation and apoptosis. Environ. Health Perspect., **110**, 757-759.

Fu, Z. and Tindall, D.J. (2008): FOXOs, cancer and regulation of apoptosis. Oncogene, **27**, 2312-2319.

Furukawa-Hibi, Y., Yoshida-Araki, K., Ohta, T., Ikeda, K. and Motoyama, N. (2002): FOXO forkhead transcription factors induce G(2)-M checkpoint in response to oxidative stress. J. Biol. Chem., **277**, 26729-26732.

Greer, E.L. and Brunet, A. (2005): FOXO transcription factors at the interface between longevity and tumor suppression. Oncogene, **24**, 7410-7425.

Hayflick, L. and Moorhead, P.S. (1961): The serial cultivation of human diploid cell strains. Exp. Cell Res., **25**, 585-621.

Ho, I.-C., Yih, L.-H., Kao, C.-Y. and Lee, T.-C. (2000): Tin-protoporphyrin potentiates arsenite-induced DNA strand breaks, chromatid breaks and kinetochore-negative micronuclei in human fibroblasts. Mutat. Res., **452**, 41-50.

Ho, K.K., Myatt, S.S. and Lam, E.W. (2008): Many forks in the path: cycling with FoxO. Oncogene, **27**, 2300-2311.

Huang, C., Ma, W.-Y., Li, J., Goranson, A. and Dong, Z. (1999): Requirement of Erk, but not JNK, for arsenite-induced cell transformation. J. Biol. Chem., **274**, 14595-14601.

Jin, S., Antinore, M.J., Lung, F.-D., Dong, X., Zhao, H., Fan, F., Colchagie, A.B., Blanck, P., Roller, P.P., Fornace, A.J.Jr. and Zhan, Q. (2000): The GADD45 inhibition of Cdc2 kinase correlates with GADD45-mediated growth suppression. J. Biol. Chem., **275**, 16602-16608.

Kops, G.J., Medema, R.H., Glassford, J., Essers, M.A., Dijkers, P.F., Coffer, P.J., Lam, E.W. and Burgering, B.M. (2002): Control of cell cycle exit and entry by protein kinase B-regulated Forkhead transcription factors. Mol. Cell. Biol., **22**, 2025-2036.

Kops, G.J., De Ruiter, N.D., De Vries-Smits, A.M., Powell, D.R., Bos, J.L. and Burgering, B.M. (1999): Direct control of the forkhead transcription factor AFX by protein kinase B. Nature, **398**, 630-634.

Lee, T.-C. and Ho, I.-C. (1995): Modulation of cellular antioxidant defense activities by sodium arsenite in human fibroblasts. Arch. Toxicol., **69**, 498-504.

Lehtinen, M.K., Yuan, Z., Boag, P.R., Yang, Y., Villén, J., Becker, E.B., DiBacco, S., de la Iglesia, N., Gygi, S., Blackwell, T.K. and Bonni, A. (2006): A conserved MST-FOXO signaling pathway mediates oxidative-stress responses and extends life span. Cell, **125**, 987-1001.

Liu, J., Kadiiska, M.B., Liu, Y., Lu, T., Qu, W. and Waalkes, M.P. (2001): Stress-related gene expression in mice treated with inorganic arsenicals. Toxicol. Sci., **61**, 314-320.

Mandal, B.K. and Suzuki, K.T. (2002): Arsenic round the world: a review. Talanta, **58**, 201-235.

Moon, K., Guallar, E. and Navas-Acien, A. (2012): Arsenic exposure and cardiovascular disease: An updated systematic review. Curr. Atheroscler. Rep., **14**, 542-555.

Nakae, J., Park, B.-C. and Accili, D. (1999): Insulin stimulates phosphorylation of the forkhead transcription factor FKHR on serine 253 through a wortmannin-sensitive pathway. J. Biol. Chem., **274**, 15982-15985.

Rossman, T.G. (2003): Mechanism of arsenic carcinogenesis: an integrated approach. Mutat. Res., **533**, 37-65.

Simeonova, P.P. and Luster, M.I. (2000): Mechanisms of arsenic carcinogenicity: genetic or epigenetic mechanisms? J. Environ. Pathol. Toxicol. Oncol., **19**, 281-286.

Storz, P. (2011): Forkhead homeobox type O transcription factors in the responses to oxidative stress. Antioxid. Redox Signal., **14**, 593-605.

Suzuki, M. and Boothman, D.A. (2008): Stress-induced premature senescence (SIPS)--Influence of sips on radiotherapy. J. Radiat. Res., **49**, 105-112.

Tran, H., Brunet, A., Grenier, J.M., Datta, S.R., Fornace, A.J.Jr., DiStefano, P.S., Chiang, L.W. and Greenberg, M.E. (2002): DNA repair pathway stimulated by the forkhead transcription factor FOXO3a through the Gadd45 protein. Science, **296**, 530-534.

Van Der Heide, L.P., Hoekman, M.F. and Smidt, M.P. (2004): The ins and outs of FoxO shuttling: mechanisms of FoxO translocation and transcriptional regulation. Biochem. J., **380**, 297-309.

Wu, M.-M., Chiou, H.-Y., Wang, T.-W., Hsueh, Y.-M., Wang, I.-H., Chen, C.-J. and Lee, T.-C. (2001): Association of blood arsenic levels with increased reactive oxidants and decreased antioxidant capacity in a human population of northeastern Taiwan. Environ. Health Perspect., **109**, 1011-1017.

Wu, M.-M., Kuo, T.-L., Hwang, Y.-H. and Chen, C.-J. (1989): Dose-response relation between arsenic concentration in well water and mortality from cancers and vascular diseases. Am. J. Epidemiol., **130**, 1123-1132.

Yoshida, T., Yamauchi, H. and Fan Sun, G. (2004): Chronic health effects in people exposed to arsenic via the drinking water: Dose-response relationships in review. Toxicol. Appl. Pharmacol., **198**, 243-252.

You, B.R. and Park, W.H. (2012): Arsenic trioxide induces human pulmonary fibroblast cell death via increasing ROS levels and GSH depletion. Oncol. Rep., **28**, 749-757.

Yuan, Z., Lehtinen, M.K., Merlo, P., Villén, J., Gygi, S. and Bonni, A. (2009): Regulation of neuronal cell death by MST1-FOXO1 signaling. J. Biol. Chem., **284**, 11285-11292.

Zanella, F., Rosado, A., García, B., Carnero, A. and Link, W. (2008): Chemical genetic analysis of FOXO nuclear-cytoplasmic shuttling by using image-based cell screening. Chembiochem, **9**, 2229-2237.